Journal of Hydrology 540 (2016) 835–849

Contents lists available at ScienceDirect

Journal of Hydrology

journal homepage: www.elsevier.com/locate/jhydrol

Research papers

Characterisation of hydraulic head changes and aquifer properties in the London Basin using Persistent Scatterer Interferometry ground motion data

R. Bonì [a,b,*], F. Cigna [a], S. Bricker [a], C. Meisina [b], H. McCormack [c]

[a] British Geological Survey, Natural Environment Research Council, Nicker Hill, Keyworth, Nottinghamshire NG12 5GG, UK
[b] Department of Earth and Environmental Sciences, University of Pavia, Via Ferrata 1, 27100 Pavia, Italy
[c] CGG, NPA Satellite Mapping, Crockham Park, Edenbridge, Kent TN8 6SR, UK

ARTICLE INFO

Article history:
Received 4 March 2016
Received in revised form 27 June 2016
Accepted 30 June 2016
Available online 1 July 2016
This manuscript was handled by P. Kitanidis, Editor-in-Chief, with the assistance of Niklas Linde, Associate Editor

Keywords:
Persistent Scatterer Interferometry (PSI)
London
Groundwater level
Chalk aquifer
Storage
Compressibility

ABSTRACT

In this paper, Persistent Scatterer Interferometry was applied to ERS-1/2 and ENVISAT satellite data covering 1992–2000 and 2002–2010 respectively, to analyse the relationship between ground motion and hydraulic head changes in the London Basin, United Kingdom. The integration of observed groundwater levels provided by the Environment Agency and satellite-derived displacement time series allowed the estimation of the spatio-temporal variations of the Chalk aquifer storage coefficient and compressibility over an area of ~1360 km^2. The average storage coefficient of the aquifer reaches values of 1×10^{-3} and the estimated average aquifer compressibility is 7.7×10^{-10} Pa^{-1} and 1.2×10^{-9} Pa^{-1} for the periods 1992–2000 and 2002–2010, respectively. Derived storage coefficient values appear to be correlated with the hydrogeological setting, where confined by the London Clay the storage coefficient is typically an order of magnitude lower than where the chalk is overlain by the Lambeth Group. PSI-derived storage coefficient estimates agree with the values obtained from pumping tests in the same area. A simplified one-dimensional model is applied to simulate the ground motion response to hydraulic heads changes at nine piezometers. The comparison between simulated and satellite-observed ground motion changes reveals good agreement, with errors ranging between 1.4 and 6.9 mm, and being 3.2 mm on average.

1. Introduction

Many cities rely on groundwater for water supply. In most parts of Europe over 40% of water supply comes from urban aquifers (Wolf et al., 2006). Monitoring and careful management of urban aquifers is needed to ensure that the aquifers are utilised in a sustainable manner and groundwater extracted for use is naturally replenished. One of the most obvious effects related to prolonged groundwater over-exploitation across city-regions is land subsidence related to falling groundwater levels and/or uplift caused by recovery of groundwater heads due to the reduction in abstraction (Morris et al., 2003; Bell et al., 2008).

Changes to the aquifers and the geological strata overlying aquifers need to be understood and quantified, such that (i) changes in groundwater levels do not cause inundation of water into underground assets, (ii) differential changes in ground saturation do not significantly affect ground engineering properties, and (iii) ground level change does not cause damage to existing infrastructure. Aquifer consolidation is commonly calculated based on Terzaghi's consolidation theory (Terzaghi, 1943). With the vertical total stress unchanged, a variation in pore-fluid pressure causes a proportional change in effective stress within the aquifer, resulting in a volume change. The latter is influenced by the compressibility of the aquifer. When the effective stress does not exceed the maximum effective stress that the system has experienced in the past (i.e. pre-consolidation stress), the fluctuations in the water level create small elastic deformation of the aquifer-system and small land surface displacement. On the contrary, if the effective stress exceeds the pre-consolidation stress, the pore structure of susceptible fine-grained aquitards in the system may undergo significant rearrangement and the deformation is mainly inelastic (Galloway et al., 1999). Vertical ground motion can therefore be the effect of the elastic and/or inelastic compaction which depends on the hydraulic head changes and the thickness of the unconsolidated deposits (Riley, 1969; Helm, 1975, 1976).

The amount of water released or stored per unit of area of the aquifer and per unit head change is defined as the storage coefficient or storativity (Fetter, 2001). This is a key property of

* Corresponding author at: Department of Earth and Environmental Sciences, University of Pavia, Via Ferrata 1, 27100 Pavia, Italy.
E-mail address: roberta.boni01@universitadipavia.it (R. Bonì).

http://dx.doi.org/10.1016/j.jhydrol.2016.06.068
0022-1694/

the aquifer system that reflects the response of aquifers and aquitards to hydraulic head changes, and is important to estimate the available groundwater resource. The storage coefficient is usually obtained either *in situ* by measuring drawdown rates during pumping tests or from lab-based porosity values. Results from pumping tests are limited in that they are representative only of the permeable portion of the aquifer within proximity of the pumping well and several assumptions about the hydraulic conditions and pumping well are made (Fetter, 2001). Validity of the results of the test is dependent on the duration of the test and the number of observation wells used to measure the aquifer response. In addition, pumping test sites are biased towards high-yielding aquifer conditions since most tests are conducted on prospective abstraction wells. Meanwhile, lab measurements have a small-sample volume, samples may be disturbed and therefore may not be representative of the *in situ* conditions (Riley, 1998). These methods are also only able to estimate this parameter for a limited number of points due to their costs, and in some cases, the results are of questionable reliability (Balkhair, 2002; Schad and Teutsch, 1994; Kaczmaryk and Delay, 2007).

During the last two decades, many studies have integrated satellite interferometric synthetic aperture radar (InSAR; Gabriel et al., 1989; Massonnet and Rabaute, 1993) and groundwater level change data to estimate the aquifer-system storage coefficient (Hoffmann et al., 2001, 2003; Galloway and Hoffmann, 2007; Bell et al., 2008; Tomás et al., 2006, 2011; Ezquerro et al., 2014; Reeves et al., 2014; Chaussard et al., 2014). Persistent Scatterer Interferometry (PSI) is an InSAR processing method that exploits significant stacks of time-stamped SAR images to identify radar targets or Persistent Scatterers (PS) on the Earth's surface for which the displacement time series along the line of sight (LOS) of the satellite is reconstructed (e.g., Ferretti et al., 2001; Werner et al., 2003; Hooper et al., 2004). The technique has been successfully used to analyse land deformation due to groundwater level variations in a number of cities and regions world-wide, such as Mexico City (Osmanoğlu et al., 2011) and Morelia in central Mexico (Cigna et al., 2012), Vega Media, Madrid, Alto Guadalentín and Granada Basins in Spain (Herrera et al., 2009; Ezquerro et al., 2014; Bonì et al., 2015; Notti et al., 2016).

In the United Kingdom (UK) the most important aquifer is the Chalk which accounts for 60% of the groundwater used in England and Wales (UK Groundwater Forum, 1998) and supports approximately 80% of public water supply in the River Thames Catchment and 20% in London (Thames Water, undated). Not only are public water supplies taken directly from groundwater, but also from surface water sources derived from rivers with a high groundwater baseflow index (BFI). The River Thames in London is one such river with a large groundwater baseflow component (BFI of 0.63 for the River Thames at Kingston gauging station 39001; NRFA, 2016). The Chalk aquifer in London has been exploited for public and industrial supply since the 1850s and is one of the most monitored and managed aquifer-systems in the UK (Jones et al., 2012; Royse et al., 2012). The chalk aquifer continues to be an important source of water for London however, a reduction in abstraction since the 1950s has led to problems with rising groundwater levels and as a result artificial recharge schemes (O'Shea and Sage, 1999; Jones et al., 2012) and open-loop ground source heating schemes (Fry, 2009) have been encouraged as part of the aquifer management schemes. The chalk aquifer is also host to increasing subsurface infrastructure such as transport tunnels, with dewatering schemes necessary to facilitate their installation (Royse et al., 2012). It is therefore essential to understand the variations of aquifer properties throughout the Chalk, in order to safeguard the groundwater resource and manage its multiple uses.

To date there have been few studies on the Chalk aquifer storage coefficient variations throughout the London Basin, although there has been a number of specific studies on the properties of the Chalk. Lewis et al. (1993) estimated the Chalk storage by using data derived from pumping tests across the whole of England. Allen et al. (1997) analysed the aquifer properties of the Chalk of England using 2100 pumping tests collated by the British Geological Survey (BGS) and the Environment Agency. However, detailed field studies are necessary to determine the physical properties of the Chalk aquifer in the London Basin, in order to take into account the site specific matrix-fracture interaction.

A recent study by Cigna et al. (2015) revealed that an area of $\sim$200 km^2 in the administrative area of Greater London ($\sim$1580 km^2) has been affected by anthropogenic land subsidence due to groundwater abstraction. In particular, these authors made use of PSI ground motion information for 1992–2000 and 2002–2010 and geological data to delineate natural and anthropogenic geohazards within the framework of the European Commission FP7-SPACE project PanGeo. Another study by Bateson et al. (2009) used PSI data of the period 1997–2005 to validate the results of the modelled subsidence due to groundwater abstraction for the Merton area of south-west London.

To date, PSI ground motion data have not been used to estimate the storage coefficient in the London Basin and to understand the spatio-temporal variability of this parameter under different aquifer conditions. For the first time, in this paper, such an analysis is undertaken by exploiting ground motion data for the years 1992–2000 and 2002–2010, obtained by processing two stacks of ERS-1/2 and ENVISAT radar imagery by using the Interferometric Point Target Analysis (IPTA) technique (Werner et al., 2003). The analysis allows the characterisation of the aquifer properties over an area of $\sim$1360 km^2. The results obtained based on the satellite ground motion observations are compared with storage coefficient records obtained *in situ* via pumping tests. Furthermore, the ground motion response to hydraulic head changes are analysed at nine piezometers.

2. Study area

2.1. Geology

The London Basin covers an area of $\sim$2500 km^2 (Fig. 1) in southern England. The basin overlies the London platform formed of Palaeozoic basement which is bounded to the south by the Variscan Front (Royse et al., 2012). The Chalk Group, which reaches thicknesses of over 200 m in central London forms a rim around younger Palaeogene deposits which infill the London Basin (Ford et al., 2010; Mathers et al., 2014). The Palaeogene strata which overlie and confine the chalk have a variable lithology and form a broad flat valley through which the River Thames flows. The Palaeogene deposits comprise, the Thanet Formation, a fine-sand unit; the Lambeth Group consisting of vertically and laterally variable sequences mainly of clay with silty and sandy horizons; the Harwich Formation a silty, sandy clay with gravel beds, and; the London Clay Formation, a dense fissured clay (Sumbler, 1996; Ellison et al., 2004). Quaternary deposits, primarily river terrace deposits associated with the River Thames and artificially modified ground, such as embankments or landfill and engineered cuttings and quarries provide a discontinuous cover at surface.

Fig. 1 shows the bedrock geology of the London Basin and the location of the main faults. It is evident that much of central London lies within a graben bounded by the Northern Boundary fault to the north and the Wimbledon-Streatham fault and the Greenwich fault to the south, where the chalk is downthrown by some 50 m. However, recent investigations by the London Basin Forum (Mortimore et al., 2011; Royse et al., 2012) and ground conditions encountered during recent engineering projects, such as the

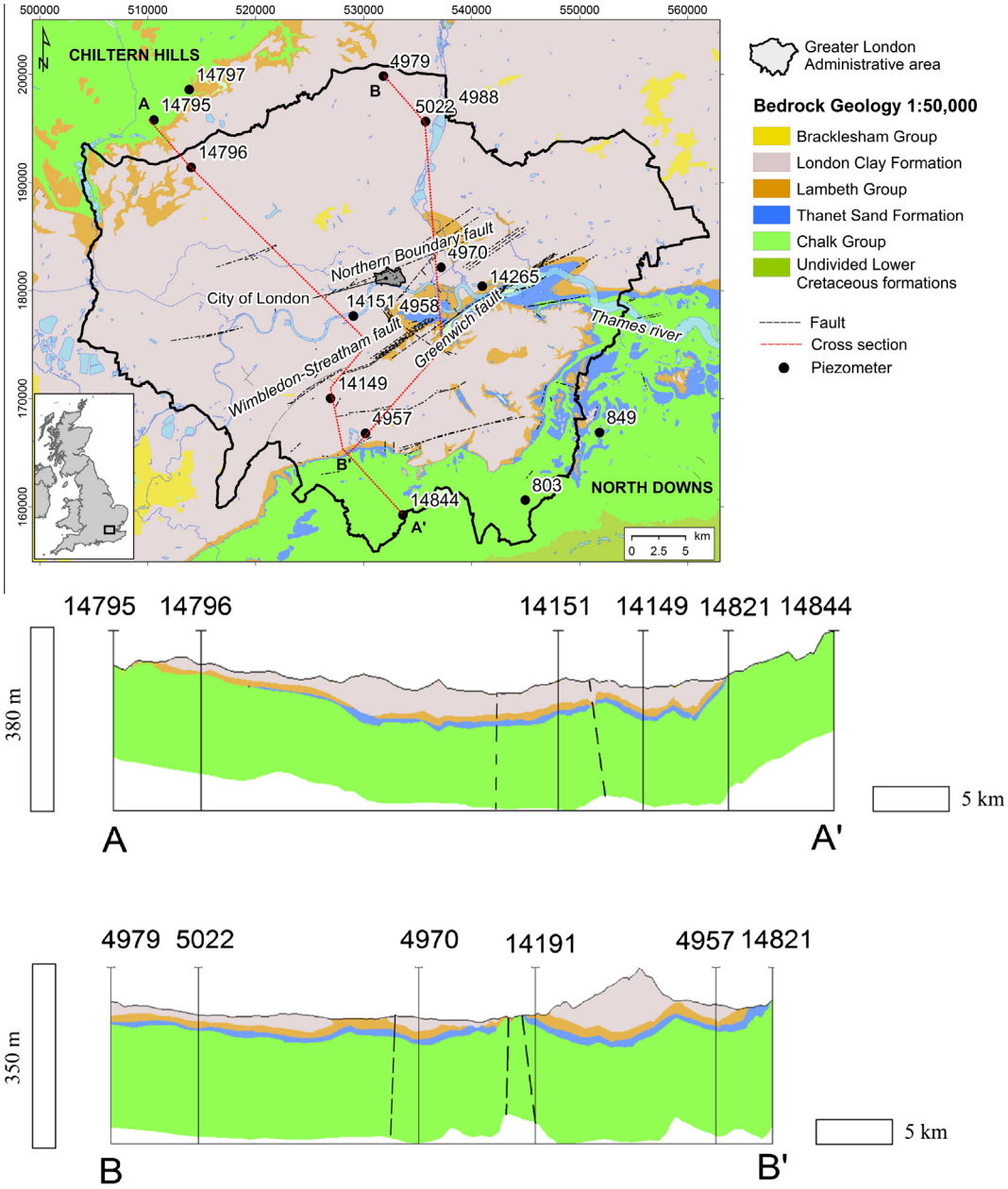

Fig. 1. Geological setting of the study area with indication of water bodies and river network from the European Urban Atlas (EEA, 2010). Geological materials © NERC. All rights reserved. Urban Atlas © Directorate-General Enterprise and Industry. British National Grid. Projection: Transverse Mercator. Datum: OSGB 1936.

Channel Tunnel Rail Link, Thames Water Ring Main (Newman, 2009), Crossrail (Aldiss, 2013) and the Docklands Light Railway, show that the geological structure of the London Basin is more complex than previously thought and faults are under-represented by current mapping (Aldiss, 2013). Reactivation of basement tectonic structures during the break-up of Pangea and the alpine orogeny (Jurassic – Tertiary) is likely to have resulted in the propagation of faults and fracture networks throughout the younger London Basin sequences, explaining significant faulting observed in the Chalk Group and overlying units during these more recent site investigations. A 3-D geological model of the Thames Valley generated by the BGS in order to visualise the distribution of the geological units along the valley (Mathers et al., 2014) has been used to extract the cross sections A-A′ and B-B′ in Fig. 1.

2.2. Hydrogeology

The Chalk Group forms a principal aquifer in the London Basin supporting public water supply (Jones et al., 2012), industrial groundwater use such as ground source heating systems (Fry, 2009) and significant baseflow to the River Thames (BFI 0.63). In the central area of the Basin, the chalk aquifer is confined by the overlying Palaeogene formations. Whilst the Palaeogene deposits do not form principle aquifers, the lithological variability within and across the units leads to hydrogeological heterogeneity and where present the sand-rich horizons can contain significant quantities of groundwater. The sand-rich Thanet Formation, for example, is highly permeable and often in hydraulic continuity with the underlying chalk aquifer. The chalk aquifer is recharged on the interfluves - in the Chiltern Hills to the north and North Downs

to the south, where the Chalk is present at surface and the aquifer is unconfined. The unconfined aquifer exhibits larger seasonal water table variations, with associated stream-head migration up dry periglacial valleys and where fracture sets exert strong linear river drainage patterns (Bloomfield et al., 2011).

The effects of faulting on the chalk aquifer and groundwater flow in the central London Basin has been highlighted in recent investigations (De Freitas, 2009; Royse et al., 2012; EA, 2015) whereby compartmentalisation of the chalk by faults and differential fault permeability leads to irregular groundwater flows and difficulties during dewatering. Both lithological variations and structural features exert significant control on aquifer properties in the Thames Basin (Bloomfield et al., 2011) and on the chalk in particular. The Chalk is a dual porosity medium, with matrix and fracture porosity (Price, 1987; Barker, 1991; Price et al., 1993). The primary porosity of the Chalk (typically 0.25–0.40) is related to the presence of the *coccoliths* in the matrix, through which the aquifer does not drain readily due to the very small pore throats (Price et al., 1976; Bloomfield et al., 1995). Instead, the groundwater storage of the aquifer is mainly derived from secondary porosity along faults, through the fractures, which are also widened by dissolution processes and long bedding planes such as marl bands and flint horizons (MacDonald and Allen, 2001). In the London Basin, permeable horizons in the overlying Thanet Formation, Lambeth Group and Harwich Formation also provide some storage capability. The specific yield for the basal sands, comprising the Thanet sands and lower-most sand units of the Lambeth Group, was found to be in the range 1×10^{-2} to 3×10^{-2} in the Lee Valley in the north of the London Basin (O'Shea and Sage, 1999).

Historic overexploitation of the Chalk aquifer for industry and manufacturing up to the 1950s led to widespread lowering of groundwater levels, reaching a depth of up to 90 m below sea-level in the central London Basin (Jones et al., 2012). As a result, the Chalk aquifer became unconfined, leading to under-drainage and desaturation of the London Clay (Jones et al., 2012; Royse et al., 2012). In the 1950s a combination of aquifer depletion, improvements in surface water quality and water storage led to a decline in groundwater abstraction and a recovery of groundwater levels at a rate of up to 3 m/year (Jones et al., 2012). As groundwater recovery and re-saturation of the London Clay could potentially have negative impacts on the foundations of structures and infrastructure in the Basin, an action plan was developed by London Underground, Thames Water and the Environment Agency (EA), i.e. the GARDIT (General Aquifer Research Development and Investigation Team) strategy. As a result, an observation borehole network within the Basin was established by the EA to monitor and manage changes in groundwater levels. Since 1999 there has been an increase in the licensed volume of abstraction of at least 3×10^6 l/d in central London (EA, 2007; EA, 2015) which has been successful in stabilising the rise of groundwater levels. As a by-product of London's rising groundwater levels an artificial recharge scheme was licensed in North London, NLARS (North London Artificial Recharge Scheme; Jones et al., 2012) to help control groundwater levels and maximise the available groundwater storage in the north part of the basin where groundwater levels were depleted (O'Shea et al., 1995; O'Shea and Sage, 1999).

Records from the observation borehole network, provide detailed time-series data to reconstruct the historical groundwater level changes across the London Basin for the 1990s and 2000s (Fig. 2) and evaluate the relationship with ground level change over the same period. In particular, 236, 166 and 214 piezometers were employed to evaluate the groundwater level changes respectively in the periods 1992–2000, 2002–2010 and 1992–2010, to match with the satellite observation periods (see Section 3).

In 1992–2000, an average groundwater level rise of 2.5 m was recorded, with 26% of the observation boreholes revealing groundwater level rises of more than 5 m. The most notable groundwater level rise mainly affects the north-west and south-east of the London Basin (Fig. 2. panel *a*). Conversely, over the second period (2002–2010), an average groundwater level fall of 0.5 m was recorded by the network, and 12% of the boreholes showed groundwater level falls exceeding 5 m, with peaks of 30–40 m. In the central area of the London Basin, an area of around 52 km^2 recorded 7 m of groundwater level lowering (Fig. 2. panel *b*).

In the whole monitored period (1992–2010), a groundwater level rise of 5 m was recorded on average across the area of interest (Fig. 2. panel *c*). The northern sector of the London Basin is characterised by a general rise of the groundwater level during the whole period from 1992 to 2010, whilst the central sector records a rise in the groundwater level from 1992 to 2000 and a subsequent fall in the period 2002–2010. The southern sector is mainly characterised by falling groundwater levels in the whole monitored period.

3. Input data and methodology

3.1. SAR data and PSI analysis

The input satellite data for this study consists of 27 ERS-1 and ERS-2 SAR scenes acquired in ascending mode along track 201, and 45 ENVISAT advanced SAR (ASAR) Image Mode IS2 scenes acquired in descending mode along track 51, both datasets characterised by nominal repeat cycle of 35 days. The first dataset covers the time interval from 19/06/1992 to 31/07/2000 and the second one from 13/12/2002 to 17/09/2010.

PSI ground motion data over the area of Greater London were obtained by using the GAMMA SAR and Interferometry software and, in particular, the IPTA algorithm (Werner et al., 2003). With the IPTA method, the temporal and spatial characteristics of interferometric signatures collected from point targets were exploited to obtain surface deformation histories, terrain heights, and relative atmospheric path delays. Following the conventional approach to PSI processing, the single-master method was used to form interferograms for each dataset (using the scenes acquired on 13/01/1997 and 11/05/2007 as masters for the ERS and ENVISAT processing, respectively), and interferometric pairs were formed with all the remaining slave scenes.

The incidence angle of the employed sensor modes for both datasets is 23° from the vertical direction, which permits the detection of 92% of vertical displacements. Assuming the occurrence of sole vertical ground motion across the Basin, LOS displacements and velocities for both datasets were projected along the vertical direction. This was done by dividing the LOS estimates by the cosine of the incidence angle, hence by 0.92, corresponding with an increase in the LOS values by 8.6% (Fig. 3. panels *a* and *b*). This assumption is justified by the generally smaller magnitude of the horizontal than vertical component of the motion in areas affected by land motion due to groundwater exploitation (e.g. Samieie-Esfahany et al., 2009; Klemm et al., 2010). Moreover, no significant horizontal component of land motion has been previously detected in London based on InSAR data (Aldiss et al., 2014; Cigna et al., 2015; Bingley et al., 2007), in fact only small-scale, fault-controlled E-W lateral movements have been detected (Mason et al., 2015).

The processing results show a total of 730,254 ERS-1/2 persistent scatterers (PS), over a processing area of ~2500 km^2, hence a target density that amounts to 292 PS/km^2. The total number of ENVISAT PS found across the 2350 km^2 processing area (slightly smaller than the ERS-1/2 area due to the different footprints of the satellite frames) amounts to 838,939, hence 336 PS/km^2.

As observed by Cigna et al. (2015), who used the same input PSI data of this study, the larger number of scenes composing the

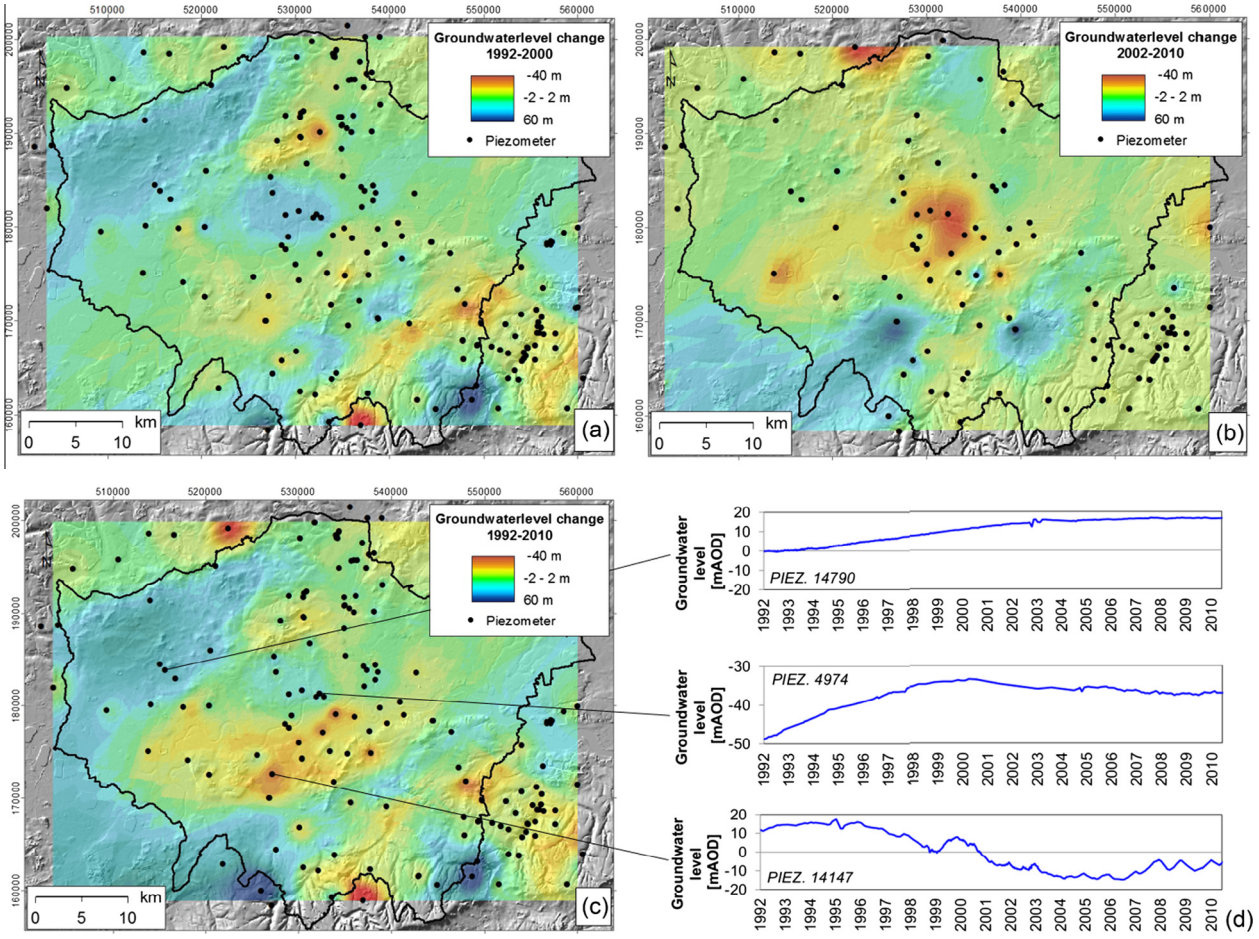

Fig. 2. Groundwater level changes in the periods (a) 1992–2000, (b) 2002–2010 and (c) 1992–2010, overlapped onto shaded relief of NEXTMap® DTM at 50 m resolution. Positive and negative values indicate, respectively, rise and fall of the groundwater level. (d) Groundwater level time series are included to illustrate different temporal changes observed across the Basin. British National Grid. Projection: Transverse Mercator. Datum: OSGB 1936. NEXTMap® Britain © 2003, Intermap Technologies Inc., All rights reserved. Groundwater level data © Environment Agency copyright and/or database rights 2015. All rights reserved.

ENVISAT stack – as opposed to the ERS one – resulted in PS datasets with denser networks of reflectors. The retrieved density of PS was also influenced by the threshold that was used for the interferometric phase standard deviation during the processing, and the resulting minimum average coherence adopted to minimise the presence of lower quality targets in the results (i.e. 0.53 for ERS and 0.49 for ENVISAT), with the ERS dataset showing less PS than the ENVISAT one, due to the higher threshold employed.

The uncertainty in the estimated ground motion velocity was also calculated during the IPTA processing and the analysis of interferometric phase residuals derived based on the iterative regression analysis to separate phase components due to linear and nonlinear deformation, topographic errors and atmospheric delay. For over 95% of the PS targets within the administrative area the uncertainty of the resulting velocities along the satellite LOS was found between 0.09 and 1.09 mm/year in the ERS-1/2 dataset, and between 0.17 and 1.13 mm/year in the ENVISAT dataset (Cigna et al., 2015).

3.2. Estimation of the aquifer storage coefficient and compressibility

The storage coefficient S or storativity represents the amount of water stored or released per unit of area of the aquifer and per unit head change. In the saturated zone, the pressure head, acts on the aquifer skeleton and on the density of the water in the pores. When the pressure increases, the aquifer skeleton expands, whilst if it decreases, the aquifer skeleton compacts (Sneed and Galloway, 2000). If the water pressure is reduced, water is released from storage in response to expansion of the water in the pores and compaction of the aquifer-system. Therefore, the aquifer-system storage coefficient S is defined as (Galloway et al., 1998):

$$S = S'_k + S_k + S_w = S^*_k + S_w \quad (1)$$

where S'_k and S_k are the skeletal storage of the aquitard and the aquifer, respectively, while S_w is the water storativity. S^*_k is the aquifer-system skeletal storage. Two aquifer-system skeletal storages, S_{ke} and S_{kv}, can be defined for the elastic and inelastic ranges of stress, respectively. The coarse-grained sediments in aquifer-systems deform elastically while the fined-grained sediments that consist on the confining aquitards may deform both elastically and inelastically.

In confined aquifers, even if the head drops and water is released from storage, the aquifer remains saturated. In this case, the storage coefficient can be defined as (Jacob, 1940; Cooper, 1966):

$$S = S_s \times b = (\rho_w \times g)(\alpha + n\beta)b \quad (2)$$

where S_s is the specific storage, b the thickness of the saturated aquifer, ρ_w the water density, g the acceleration of gravity, α the aquifer skeleton compressibility, n the porosity and β the fluid compressibility (approximately of 4.9×10^{-10} Pa^{-1}).

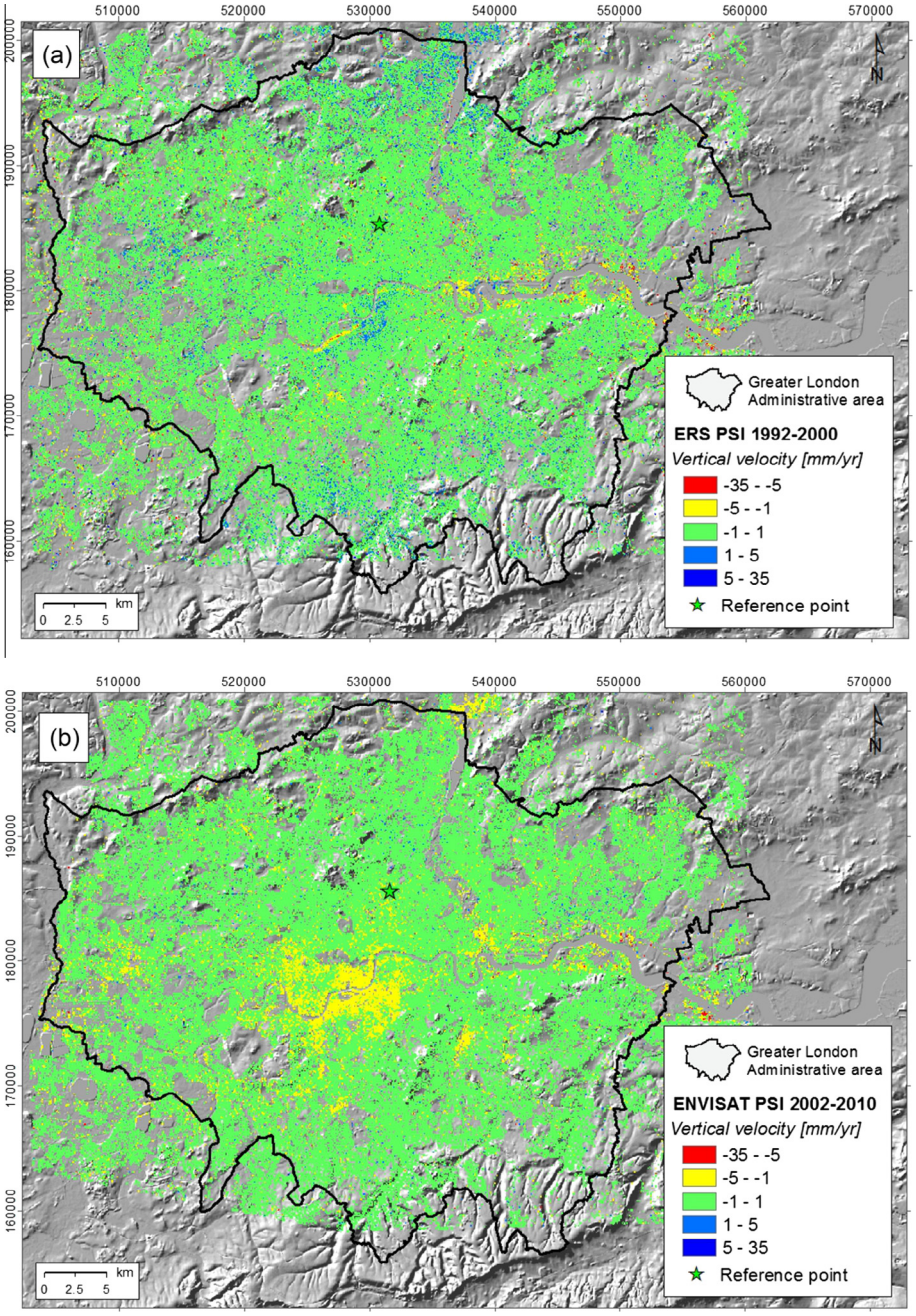

Fig. 3. Vertical motion velocities estimated for the London Basin with PSI analysis in (a) 1992–2000 and (b) 2002–2010, overlapped onto shaded relief of NEXTMap® DTM at 50 m resolution. British National Grid. Projection: Transverse Mercator. Datum: OSGB 1936. ERS-1/2 and ENVISAT PSI data © CGG NPA Satellite Mapping. NEXTMap® Britain © 2003, Intermap Technologies Inc., All rights reserved.

Note that, in compacting aquifer systems $S_k^* \gg S_w$ and, assuming that S_w is negligible (Poland, 1984) the storage coefficient is approximatively equal to the skeletal storage coefficient: $S \approx S_k^*$.

To a first approximation, for this study, S_w is assumed as negligible in the Chalk aquifer, since that the water storage is generally more than one order of magnitude lower than the specific storage (Price, 1987).

By inspecting groundwater level variations and ground displacement time series for nine boreholes across the network, stress-strain curves were derived by plotting the hydraulic head (that represents the applied stress) versus the vertical displacement (that represents the strain). Fig. 4 shows the strain reaction to the most evident cycles of loading and unloading of the stress (hydraulic head) at three piezometers where significant hydraulic head changes were observed. The results show a recovery of the strain corresponding with the stress dissipation. A direct temporal correlation between start and end dates for rising water level and ground uplift, and falling level and subsidence was found. As a consequence, taking into account the linear correlation observed between groundwater level changes and displacements, the deformational behaviour of the aquifer was considered as mainly elastic (hence well described by S_{ke}), which is consistent with previous investigations highlighting the importance of elastic storage for both the confined and unconfined chalk (MacDonald and Allen, 2001). This suggested that the hydraulic head changes produced an instantaneous effect on the aquifer pore pressure.

In the London Basin, the aquifer exhibits semi-confined and confined conditions for ~1360 km^2 of the study area. Similarly to

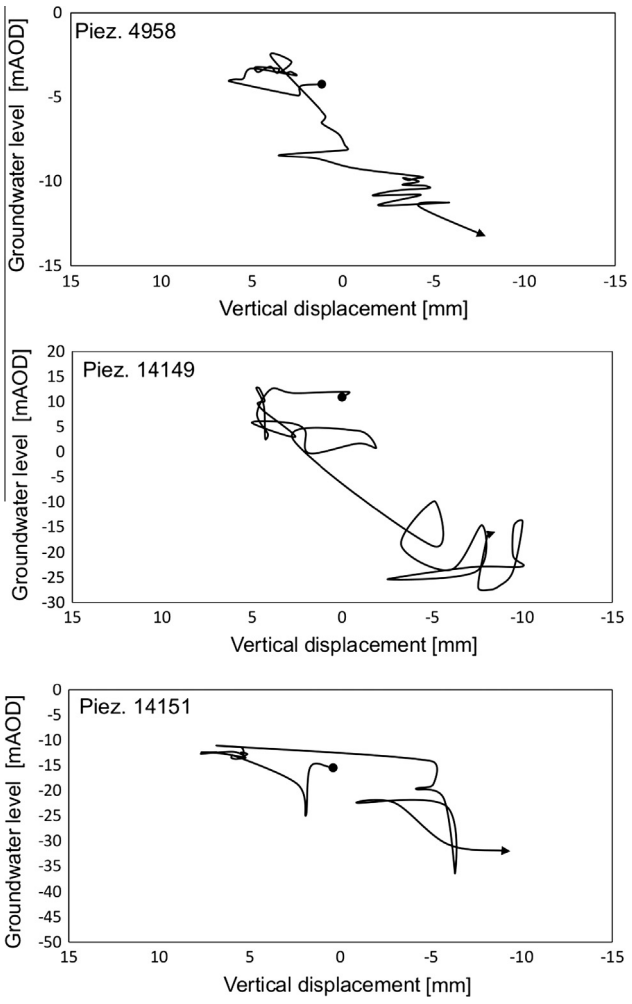

Fig. 4. Stress-strain curve at three piezometers. See location in Fig. 1 and piezometers time series in Fig. 5.

the methodology that other authors have implemented for different aquifer-systems (Hoffmann et al., 2003; Bell et al., 2008; Tomás et al., 2006; Chaussard et al., 2014), for this area, the relationship between the hydraulic heads changes and the vertical ground motion changes was applied to compute the storage coefficient (Hoffmann et al., 2001):

$$S = S_k^* = \Delta d/\Delta h \tag{3}$$

where Δd is the vertical displacement as estimated by the satellite data, and Δh is the hydraulic head change. Note that this equation assumes that ground deformation is only vertical, a hypothesis that is justified by the fact that the horizontal displacements are believed to be not significant for this area.

The Chalk aquifer properties are mainly the result of the fracture network throughout its thickness, and the contribution from the matrix porosity is largely lower than that from the fractures (see Section 2). Eq. (2) can be therefore expanded to (Price, 1987):

$$S_s = \rho_w g(\alpha_f + \alpha_m + n_f\beta + n_m\beta) \tag{4}$$

where α_f is the compressibility of the aquifer due to the presence of fractures, α_m is the compressibility of the aquifer skeleton unfractured, n_f represents the porosity resulting from the fractures, n_m is the matrix porosity, and $(n_f\beta + n_m\beta)$ indicates the specific storage of water S_{sw}.

As the latter is negligible, the total compressibility of the Chalk aquifer α can therefore be computed as:

$$\alpha = \alpha_f + \alpha_m = S_s/\rho_w g \tag{5}$$

4. Results and discussion

4.1. Modelling ground motion caused by groundwater level change

A simple 1-D model based on the inversion of Eq. (3) by Hoffmann et al. (2001) has been used to estimate the vertical displacement of the ground in response to changes in hydraulic head in the chalk aquifer. The model is used to characterise the relationship between groundwater level and ground motion time-series data to assess the contrast in ground motion across different geological units and in different aquifer conditions.

The 1-D model assumes that the aquifer pore pressure instantaneously equilibrates with piezometric level changes in the aquifer and any time-lag between the piezometer level variations and the compaction of the geological layers is not accounted for. This assumption is supported by our inspection of the ground motion and groundwater records for boreholes across the Basin (see Section 3.2). As applied by other authors (Tomás et al., 2010; Ezquerro et al., 2014) to predict the ground motion changes due to groundwater level variations, in this study the simulated displacements were quantified by inverting Eq. (3) as:

$$\Delta d = S \times \Delta h \tag{6}$$

The relationship between hydraulic head changes that occurs from 1992 to 2010 and the vertical displacement detected by PSI data for nine piezometers (see the localisation in Fig. 1) was analysed. Note that whilst the simulated displacements are only referred to ground motion due to measured groundwater level changes, PS measurements indicate the total motion for any given point, which can be due to several processes (including anthropogenic factors, e.g. engineering works, or natural processes, e.g. compaction of soft sediments). If not accounted for, this could lead to an over-estimation of the storage. In order to minimise the influence of ground motion triggered by other factors on the estimation of the aquifer storage, in this study PS time series showing unrelated motion patterns and rates, for instance, high rates of uplift or land subsidence due to other processes as identified by the geohazard mapping carried out during the project PanGeo (Cigna et al., 2015) were first excluded from the analysis. Moreover, the average vertical displacement based on the remaining time series was estimated by using buffer areas with a radius of 500 m from each piezometer. For each piezometer at least 10 PS time series were used. Groundwater level data of ~200 piezometers were then compared with the average vertical displacement of the time series within each buffer area.

The aquifer storage coefficient S was calculated by using Eq. (3) in the time interval where a good fit between piezometer data and average displacement time series was evident. The summary of storage coefficients computed for the nine boreholes are displayed in Table 1. In addition, the absolute average error between the simulated and PSI-derived displacements was estimated.

For each piezometer the geological sequence was compared with the groundwater level variation to classify the aquifer state according to its confined condition (i.e. confined, semi-confined, unconfined) and the geological interval over which the piezometric head varied (Table 1). The same approach of storage coefficient computation that was applied in the confined aquifer condition was extended to estimate the storage coefficient in semi-confined conditions, in which storage within the confining unit is considered important (Burbey, 2003). Note that a transition between confined and unconfined conditions was detected at piezometer 14265 (Fig. 5) and two different storage coefficients were estimated for the different aquifer conditions in the periods

Table 1
Summary of the piezometers where displacements were simulated. *Piez.ID*, unique code of each piezometer, *S*, storage coefficient. Note that the calibration period was chosen based on visual identification of good fit between groundwater level and displacement time series. Shrink-swell hazard ratings are from BGS GeoSure dataset, and refer to the predominant ratings observed within the 500 m buffer area around each borehole. Volume Change Potential (VCP) ratings and plasticity index (I_p) values for the London Clay are from Jones and Terrington (2011) and do not account for plasticity variations with depth. VCP indicates the relative change in volume to be expected with soil moisture content changes.

Location	Piez. ID	Calibration period	Aquifer condition	Geological unit within which the hydraulic head fluctuates	Groundwater level change (m)	Ground level change (mm)	*S*	Average error (mm)	Thickness of the Lambeth Group (m)	Thickness of clay deposits (m)	Shrink-swell hazard	VCP (I_p)
Northern London Basin	4979	04/03/99–09/09/99	Semi-confined	Lambeth Group	−1.98	−2.93	1.48×10^{-3}	3.10	29.10	17.00	D	High (45)
	4988	26/06/03–17/11/03	Confined	Lambeth Group	−11.50	−5.85	5.08×10^{-4}	2.62	–	37.00	D	High (45)
	5022	17/10/97–05/03/98	Confined	London Clay	1.47	0.74	5.05×10^{-4}	3.15	9.80	8.00	D and A	High (50)
Central London Basin	14265	01/02/96–12/12/97	Confined	Silicate-gravel	12.16	4.49	3.69×10^{-4}	1.65	15.60	6.70	C	–
		14/01/04–13/12/04	Semi-confined	Alluvium Silicate-clay	−2.32	−6.14	2.65×10^{-3}					
	4970	02/04/96–14/12/98	Confined	London Clay	6.43	2.93	4.55×10^{-4}	2.34	16.40	24.70	D and A	Medium (37)
	4958	15/07/92–30/03/00	Semi-confined	Lambeth Group	2.45	2.85	1.16×10^{-3}	2.00	8.23	0	A and B	–
Southern London Basin	14149	07/06/96–27/09/99	Confined	London Clay	−13.16	−6.92	5.26×10^{-4}	6.92	9.50	47.00	D	High (47)
	14151	03/05/95–20/12/99	Confined	London Clay	1.04	0.77	7.44×10^{-4}	6.05	8.50	39.00	C and D	High (40)
	4957	15/02/08–15/10/08	Confined	London Clay	−5.77	−2.76	4.78×10^{-4}	1.40	24.00	30.00	D and A	High (49)

01/02/1996–12/12/1997 and 14/01/2004–13/12/2004 respectively for the confined and semi-confined conditions.

Fig. 5 shows the simulated displacements at six piezometers in order to represent the main ground motion responses to hydraulic head changes in the different states of the aquifer. These are obtained by using the groundwater level data and the estimated storage coefficients as inputs to Eq. (6).

In the North London Basin, the aquifer exhibits both confined and semi-confined conditions, varying spatially and occasionally temporally. When the piezometric level is within the Lambeth Group, a hydraulic head change of around 1.98 m corresponds to 2.93 mm of surface displacement (Fig. 5; piezometer 4979). When the Chalk is confined by the London Clay, the hydraulic head change of 11.50 m produces approximately 5.85 mm of surface displacement (Fig. 5; piezometer 4988).

In the Central London Basin, temporary transition of the water table across the units was detected (Fig. 5; piezometer 14265). In this case, the simulated displacement was estimated using two storage coefficient values, taking into account the groundwater level variations in the lithological units.

In the South London Basin, the aquifer is confined by thicker deposits of the London Clay and lower values of storage coefficient were detected. Hydraulic head change of 13.16 m produces around 6.92 mm of surface displacement (Fig. 5; piezometer 14149).

A correlation between the derived storage coefficient and the aquifer condition is also observed (Table 1). Where the chalk is confined by the London Clay the storage coefficient is of the order of 1×10^{-4}, whilst where overlain by the Lambeth Group and semi-confined condition are expected to exist the storage is higher, typically 1×10^{-3} and indicative of additional storage provided by sand-rich horizons in the Lambeth Group.

Also note that the absolute average difference error between the simulated and PSI-derived displacement shows higher values where the clay deposit is thicker (Table 1), and this fact could be due to swelling and shrinking of the London Clay deposits which have a high plasticity (e.g. Freeborough et al., 2006; Jones and Terrington, 2011). To take into account the possible influence of shrink-swell clays on the observed errors, the BGS GeoSure dataset that provides information about potential natural ground movement resulting from collapsible deposits, compressible ground, landslides, running sand, shrink-swell and soluble rocks, by using A (lowest) to E (highest) ratings for each of these six geohazards (BGS, 2014) was also analysed. This dataset is mapped at the 1:50,000 scale, and a 50 m buffer around the location or area of interest is generally recommended for its correct use. For this reason, GeoSure ratings for each piezometer (Table 1) were extracted as the predominant ratings observed within the 500 m buffer around each piezometer location, not only to account for this recommendation but also to be consistent with the radius used around each piezometer for the time series analysis. The Volume Change Potential (VCP) and plasticity index (I_p) of the London Clay as estimated by Jones and Terrington (2011) based on the BGS National Geotechnical Properties Database and index test data for the London Clay outcrop were also considered.

The analysis revealed that the majority of the boreholes in Table 1 are located in areas with A to D shrink-swell hazard rating, indicating ground conditions ranging from non-plastic (A) to high plasticity (D). It is worth noting that since the VCP refers to the mean plasticity index at each sample location and GeoSure hazard ratings mainly to surface geology, it is crucial to consider the effect of the different thickness of the clay deposit at the specified locations when analysing the resulting errors. For those piezometers showing a predominant rating of D and presence of thicker clay deposits, the occurrence of shrink-swell in the active zone (i.e. generally, the first ~1.5 m; Jones and Terrington, 2011) where soil

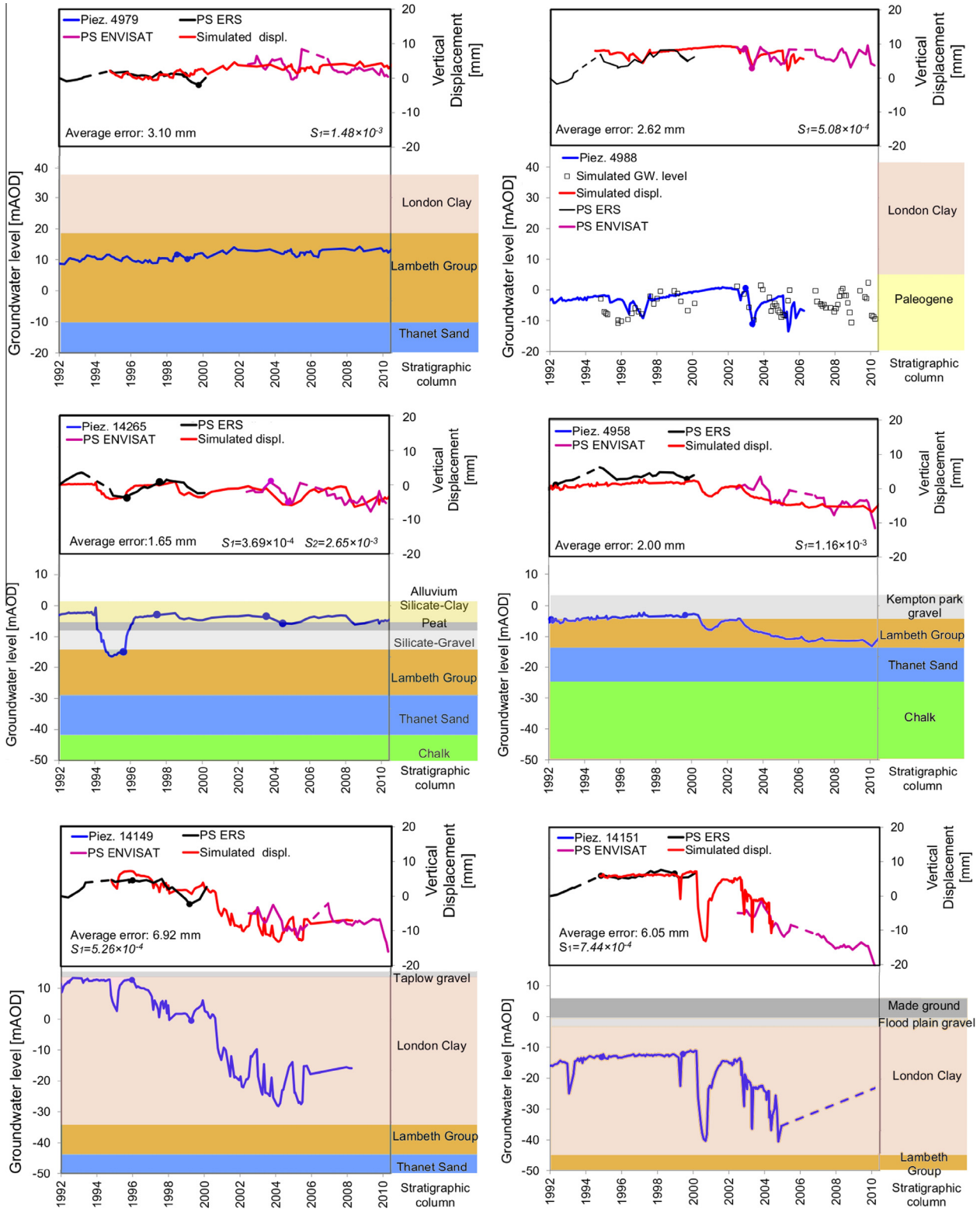

Fig. 5. Comparison of InSAR ground motion data for 1992–2000 and 2002–2010 and simulated displacements (mm) with the groundwater level variations (m). In addition, the stratigraphic column is represented. The dots represent the start and the end of the calibration period for the simulation. Piezometer localisation is in Fig. 1. For piezometer 4988, the simulated groundwater (GW) level is also reported. Groundwater level data © Environment Agency copyright and/or database rights 2015. All rights reserved.

moisture changes are more likely to occur, could partly justify the higher errors observed after the simulation.

To simulate the hydraulic head changes based on the observed ground motion, additionally Eq. (3) at piezometer 4988 was inverted (Fig. 5) as:

$$\Delta h = \Delta d / S \tag{7}$$

This approach could be used to infer groundwater level changes based on satellite ground motion data and aquifer storativity in areas of London where no observation boreholes are available.

The relative error between the simulated hydraulic head changes and the measured groundwater level variations is 25% of the hydraulic head change.

The 1-D ground motion modelling also allowed the estimation of the cumulated vertical displacement occurred between the last ERS-1/2 image (31/07/2000) and the first ENVISAT image (13/12/2002) at the nine piezometers. The ENVISAT ground motion time series in Fig. 5 were indeed adjusted for the position of the ground on 13/12/2002 to match with the modelled ground motion time series based on the ERS data. A vertical displacement of −5 mm was observed for piezometer 14149, 4 mm for piezometer 4979 and −2 mm for piezometer 14265.

4.2. Chalk aquifer properties derived from PSI data

The aim of this study is to understand the aquifer ground motion response to hydraulic head changes in the London Basin, using PSI data which spanned the periods 1992–2000 and 2002–2010. The groundwater observation network of the Environment Agency was exploited. Of the available 440 piezometers sampling the aquifer, only ~200 have got hydraulic head measurements from 1992 to 2010 (i.e. the time span of the PSI data) and were used for the comparison with the ground motion time series.

4.2.1. Confined and semi-confined aquifer properties

For this analysis, first the groundwater level changes for the periods 1992–2000 and 2002–2010 from the borehole observation network was quantified. Secondly, the average ground motion change in the two periods, detected by the PS included in a 500 m buffer area around each piezometer, was computed to account for the zone of influence of pumping. For each of these buffer areas, on average, ~200 PS were found, and the standard deviation of their vertical displacements reached maximum values of 5×10^{-2} mm, confirming the high consistence of the considered time series around each borehole.

Then, the storage coefficient was estimated using Eq. (3) for each of these boreholes by comparing the observed ground motion changes in 1992–2000 and 2002–2010 versus the hydraulic head changes measured for the same periods. Only piezometers for which a correlation between deformation and hydraulic head changes was evident were used for the following analysis. In particular, the piezometers where either groundwater level decline corresponded to observed subsidence in the ground motion data, or groundwater level rise corresponded to uplift were selected. Conversely, the piezometers where the correlation was not evident were those where ground motion is caused by others factors, such as the compressible soil compaction, neo-tectonics and near-surface fault displacements, or loading from new buildings that were documented in the literature (Aldiss et al., 2014; Cigna et al., 2015; Bingley et al., 2007). Note that no time-lag for each geological unit to compact/expand in response to the decline/increase in groundwater levels was accounted for, because none was identified during the comparison between groundwater level variations and ground motion changes for the analysed boreholes in the semi-confined and confined aquifer conditions.

By using this approach, the storage coefficient at 56 and 23 piezometers, respectively for the period 1992–2000 and 2002–2010 was obtained. Fig. 6 shows the interpolated maps of the storage coefficient, using the Inverse Distance Weighting approach. The resulting storage coefficient estimated in 1992–2000 ranged from 4.51×10^{-5} to 7.31×10^{-3}, and in 2002–2010 from 1.30×10^{-4} to 1.03×10^{-2}. In the period 1992–2000, the storage distribution highlights a mean value of 1.18×10^{-3} and median of 4.99×10^{-4}, and the 25 and 75 percentiles are 3.03×10^{-4} and 1.20×10^{-3}. The storage in the period 2002–2010 detains a mean value of 1.68×10^{-3} and median of 1.35×10^{-3}, and the 25 and 75 percentile are 4.39×10^{-4} and 2.13×10^{-3} respectively.

The values of the PSI-derived storativity maps were compared with the storage coefficient obtained by pumping tests performed in the Chalk aquifer by Allen et al. (1997) during the 1990s (see the localisation in Fig. 6). The map of the storage coefficient estimated

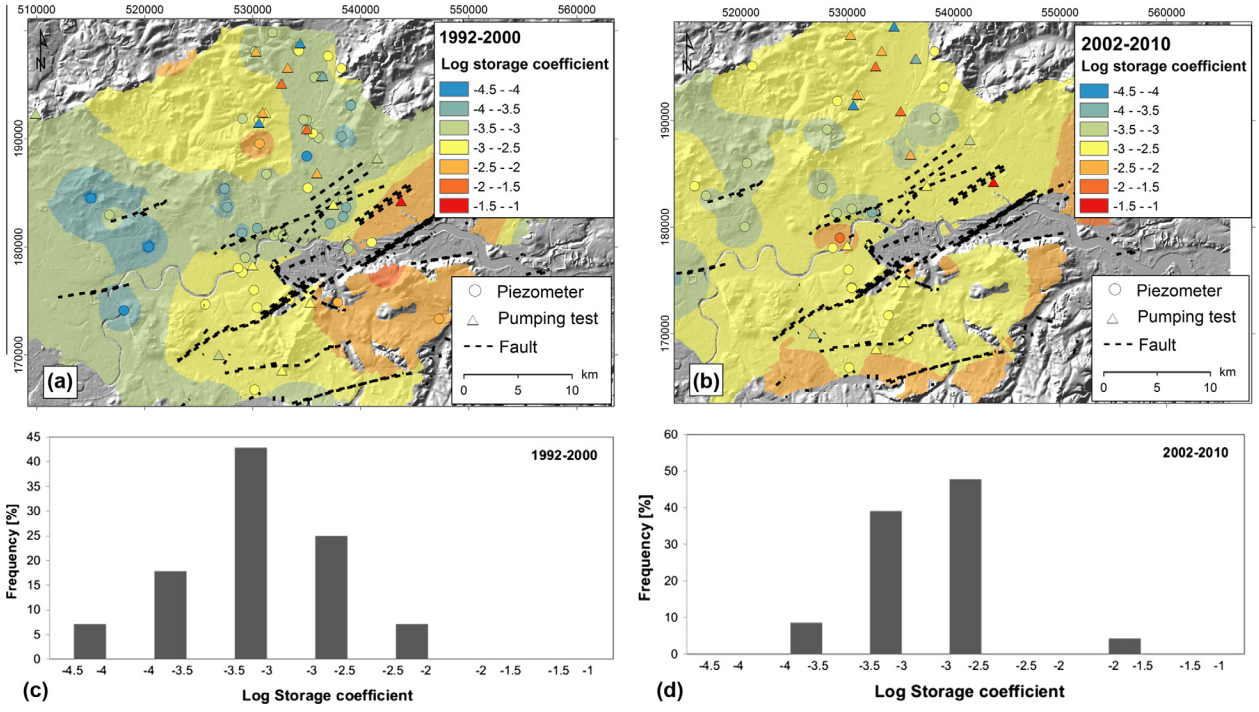

Fig. 6. Maps of the aquifer storage coefficient in (a) 1992–2000 and (b) 2002–2010 (BGS ©NERC. All Rights Reserved. 2016) overlapped onto shaded relief of NEXTMap® DTM at 50 m resolution. British National Grid. Projection: Transverse Mercator. Datum: OSGB 1936. NEXTMap® Britain © 2003, Intermap Technologies Inc., All rights reserved. Distribution of aquifer storage coefficient data in 1992–2000 (c) and 2002–2010 (d) within the London Basin.

in the period 1992–2000 was compared with the storage coefficient measured by 19 pumping tests and the second one was cross-compared by 18 pumping tests that matched with the extension of the PSI-based storage coefficient maps. The storage coefficient measured by pumping tests ranged from 9.00×10^{-5} to 5.17×10^{-2}. The storage distribution highlights a mean value of 6.85×10^{-3} and median of 2.00×10^{-3}, and the 25 and 75 percentiles are 5.00×10^{-4} and 5.40×10^{-3}. The comparisons were performed by extracting values from the PSI-based storage coefficient map values at the pumping tests locations. Table 2 cross-compares the values from the pumping tests and PSI-based assessment. PSI-based storage values for the analysed pumping test locations are between 3.53×10^{-4} and 4.88×10^{-3}, and their absolute differences with respect to the values obtained by pumping tests range between 2.20×10^{-5} and 4.91×10^{-2}. In most cases, the storage measured by pumping tests and the corresponding PSI-based values also show the same order of magnitude as confirmed by their ratios, and only a few outliers from this pattern can be observed.

Pumping tests of high reliability were used for this analysis. Indeed, only the values obtained from constant rate tests carried out for more than a day were considered, in order to minimise the error of the measured storage coefficient. It is worth noting, however, that some of the pumping tests may have been conducted within the aquifer in unconfined conditions, whereas at the present the water levels have risen and in the large part of the London Basin the aquifer is confined or semi-confined. Therefore, local differences between the two storage coefficient estimations may be justified by the change in aquifer conditions.

Taking into account that the water storage was assumed negligible, the PSI-derived storage coefficient is in good agreement with those obtained by pumping tests.

Using the method outlined previously the aquifer state and geological interval over which the change in piezometric head occurred was determined for each of the 56 piezometers used to calculate storage over the period 1992–2000. In doing so the spatial correlation between storage coefficient and aquifer condition is further assessed. Where the chalk is confined by the London Clay a storage coefficient of 1.00×10^{-4} to 1.00×10^{-5} is typically observed. The exception to this occurring near Battersea where the storage coefficient for a cluster of sites is unusually high and of the order of 1.00×10^{-3} this area coincides with the location of a number of anomalous buried hollows where ground disturbance due to peri-glacial processes is observed (Hutchinson, 1980; Banks et al., 2015). Where the chalk is overlain by the Lambeth Group and semi-confined conditions may persist higher storage values in the range 1.00×10^{-3} to 1.00×10^{-4} were observed.

Furthermore, the specific storage was calculated by inverting Eq. (2) as follows:

$$S_s = S/b \tag{8}$$

To this aim, the thickness of the Chalk (which ranges from 75 to 200 m in the region of interest) as calculated by BGS based on borehole data, was used. The resulting specific storage reaches values higher than 3.00×10^{-5} m^{-1} near the Greenwich fault (see the location in Fig. 1). The average specific storage that was estimated for the London Basin is of 7.50×10^{-6} and 1.00×10^{-5} m^{-1} respectively for the period 1992–2000 and 2002–2010. These values show good agreement with those that can be computed by using Eq. (4) and for values of matrix porosity (n_m) of 0.29, porosity contributed by the discontinuities (n_f) of 1.00×10^{-2}, compressibility of the aquifer resulting from the discontinuities (α_f) of 5.00×10^{-10} Pa^{-1}, compressibility of the unfractured matrix (α_m) of 8.10×10^{-11} Pa^{-1} and fluid compressibility (β) of 4.90×10^{-10} Pa^{-1}, resulting in 7.00×10^{-6} m^{-1} specific storage (Price, 1987).

The aquifer compressibility varies from 2.60×10^{-11} to 8.60×10^{-9} Pa^{-1} with an average of 7.70×10^{-10} Pa^{-1} in the period 1992–2000, whilst in 2002–2010, the values range from 6.40×10^{-11} to 5.70×10^{-9} Pa^{-1}, with an average of 1.20×10^{-9} Pa^{-1} (Fig. 7).

The estimated values in the first period agree with the range obtained by using the Young modulus derived from seismic surveying: 3.10×10^{-10}–8.00×10^{-10} Pa^{-1} (Abbiss, 1979). The average value obtained for the second period is also comparable with the results derived from tank test: 4.80×10^{-10}–1.20×10^{-9} Pa^{-1} (Ward et al., 1968).

4.2.2. Unconfined aquifer properties

In order to analyse the ground motion response to hydraulic head changes in the unconfined condition of the Chalk aquifer, local comparisons for the piezometers located in the Chilterns and North Down areas were carried out. In the Chiltern Hills (see Fig. 8; piezometer 14796) the long-term seasonal trend of the water table is related to the wet and dry periods. The rise and/or fall of the water table of around 2 m correspond to 4 mm in ground motion. Around five months of time lag can be observed between

Table 2
Storage coefficient estimated by pumping test (S_{pt}) and by PSI-based method (S_{PSI}).

Name	S_{pt}	S_{PSI} (1992–2000)	S_{PSI} (2002–2010)	Absolute difference ($S_{pt} - S_{PSI}$) 1992–2000	Absolute difference ($S_{pt} - S_{PSI}$) 2002–2010	Ratio (S_{pt}/S_{PSI}) 1992–2000	Ratio (S_{pt}/S_{PSI}) 2002–2010
Vauxhall bridge rhm	1.91×10^{-3}	1.29×10^{-3}	4.88×10^{-3}	6.25×10^{-4}	2.97×10^{-3}	1.49	3.91×10^{-1}
Ponders end abh no. 1	3.20×10^{-4}	4.21×10^{-4}	1.65×10^{-3}	1.01×10^{-4}	1.33×10^{-3}	7.60×10^{-1}	1.93×10^{-1}
Ponders end abh no. 2	3.00×10^{-4}	4.32×10^{-4}	1.67×10^{-3}	1.32×10^{-4}	1.37×10^{-3}	6.94×10^{-1}	1.80×10^{-1}
Park ps	2.00×10^{-2}	4.42×10^{-4}	1.76×10^{-3}	1.96×10^{-2}	1.82×10^{-2}	45.25	11.38
Hadley road	3.60×10^{-3}	6.93×10^{-4}	1.32×10^{-3}	2.91×10^{-3}	2.28×10^{-3}	5.19	2.72
Merton abbey ps	1.00×10^{-3}	1.53×10^{-3}	3.02×10^{-3}	5.27×10^{-4}	2.02×10^{-3}	6.55×10^{-1}	3.31×10^{-1}
East ham ps	5.17×10^{-2}	4.04×10^{-3}	2.63×10^{-3}	4.77×10^{-2}	4.91×10^{-2}	12.80	19.66
Old ford ps	3.00×10^{-3}	1.10×10^{-3}	2.72×10^{-3}	1.90×10^{-3}	2.82×10^{-4}	2.73	1.10
Selhurst well	2.00×10^{-3}	2.10×10^{-3}	3.13×10^{-3}	9.80×10^{-5}	1.13×10^{-3}	9.53×10^{-1}	6.39×10^{-1}
Lee bridge well no. 2	5.00×10^{-3}	1.17×10^{-3}	2.26×10^{-3}	3.83×10^{-3}	2.74×10^{-3}	4.26	2.21
Honor oak	2.40×10^{-3}	3.03×10^{-3}	3.40×10^{-3}	6.29×10^{-4}	1.00×10^{-3}	7.92×10^{-1}	7.05×10^{-1}
Myddleton road	9.00×10^{-5}	2.56×10^{-3}	2.03×10^{-3}	2.47×10^{-3}	1.94×10^{-3}	3.52×10^{-2}	4.44×10^{-2}
Wanstead	5.00×10^{-4}	1.81×10^{-3}	2.04×10^{-3}	1.31×10^{-3}	1.54×10^{-3}	2.77×10^{-1}	2.45×10^{-1}
Turkey brook	1.00×10^{-4}	8.19×10^{-4}	1.55×10^{-3}	7.19×10^{-4}	1.45×10^{-3}	1.22×10^{-1}	6.46×10^{-2}
Southbury road	5.40×10^{-3}	8.86×10^{-4}	1.44×10^{-3}	4.51×10^{-3}	3.96×10^{-3}	6.09	3.74
Oakthorpe road	1.90×10^{-3}	2.07×10^{-3}	1.92×10^{-3}	1.73×10^{-4}	2.20×10^{-5}	9.17×10^{-1}	9.89×10^{-1}
Knap arms bridge	1.00×10^{-2}	2.16×10^{-3}	1.98×10^{-3}	7.84×10^{-3}	8.02×10^{-3}	4.64	5.05
Bush hill road	2.00×10^{-2}	9.81×10^{-4}	1.46×10^{-3}	1.90×10^{-2}	1.85×10^{-2}	20.39	13.73
Hms warrior no. 2	1.00×10^{-3}	3.53×10^{-4}	–	6.47×10^{-4}	–	2.83	–

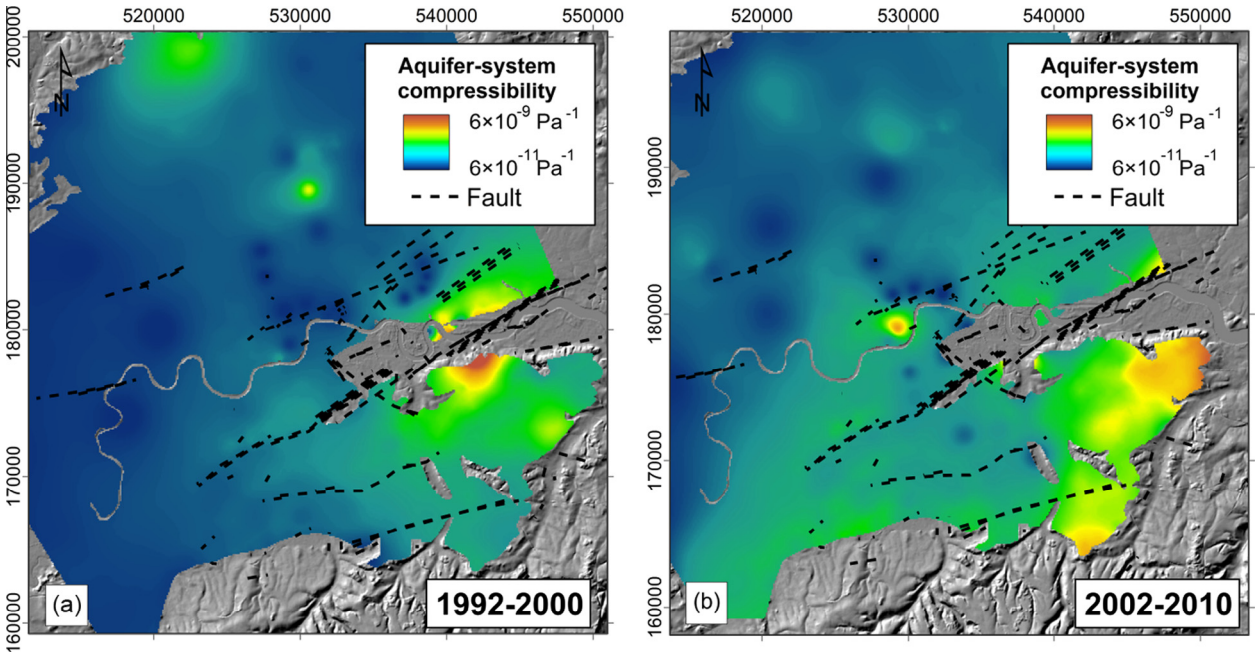

Fig. 7. Maps of the aquifer compressibility in the periods (a) 1992–2000 and (b) 2002–2010 (BGS ©NERC. All Rights Reserved. 2016), overlapped onto shaded relief of NEXTMap® DTM at 50 m resolution. British National Grid. Projection: Transverse Mercator. Datum: OSGB 1936. NEXTMap® Britain © 2003, Intermap Technologies Inc., All rights reserved.

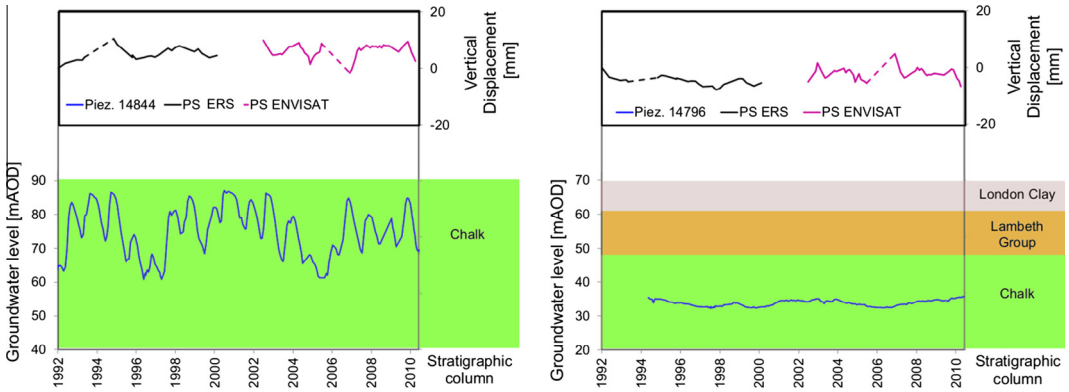

Fig. 8. Comparison of water table changes with ground motion changes at piezometers station 14844 and 14796. See Fig. 1 for the localisation. Groundwater level data © Environment Agency copyright and/or database rights 2015. All rights reserved.

the water table variations and ground motion changes at two piezometer locations (see Fig. 1; piezometers 14795 and 14796) in the Chiltern area. This time lag could be caused by the presence of a thick unsaturated zone and deposits with a low vertical hydraulic conductivity at these locations, which delays groundwater recharge. However, based on the temporal sampling frequency of the processed ERS-1/2 and ENVISAT radar imagery and the resulting time series, there is insufficient evidence to confirm the presence of this lag in other locations and its persistence across the entire monitored period 1992–2010. The observed time lag at these two piezometers could therefore simply be due to intrinsic characteristics of the satellite data time series.

In the North Downs, where the Chalk aquifer outcrops, significant seasonal rises and falls of the groundwater level are evident (see Fig. 8; piezometer 14844). Two seasonal components due to (1) short-term variations (from March to November) and to (2) long-term variation (multi-annual) were recognised. The hydraulic change of 20 m corresponds to approximately 3 mm of surface displacements.

5. Conclusions

The hydraulic properties of the Chalk aquifer have been previously investigated by several authors with traditional field and laboratory measurements and experiments (Ward et al., 1968; Carter and Mallard, 1974; Bell, 1977; Abbiss, 1979; Price, 1987; Barker, 1991; Lewis et al., 1993; Price et al., 1993; Allen et al., 1997). Although the characterisation of the Chalk aquifer properties resulting from the presence of discontinuities ideally requires estimation *in situ* over wide areas, the high costs of such campaigns only permitted to carry out investigations at limited spatial or temporal scales.

In this study, the combined analysis of hydrological information with displacement maps and time-series retrieved from multi-sensor and multi-temporal SAR images and PSI analysis has allowed the derivation of:

(1) the Chalk aquifer storage coefficient maps over an area of ~1360 km^2 in the periods 1992–2000 and 2002–2010; and

(2) the 1-D modelling of the ground motion response to hydraulic head changes at nine piezometers.

The resulting storage coefficient estimated in the period 1992–2000 ranged from 4.51×10^{-5} to 7.31×10^{-3}, and in the period 2002–2010 ranged from 1.30×10^{-4} to 1.03×10^{-2}. Additionally, these maps were compared with the storage coefficient obtained by pumping test performed in the Chalk aquifer by Allen et al. (1997) during the 1990s. The maps of the storage coefficient estimated in the periods 1992–2000 and 2002–2010 were compared with the storage coefficient measured respectively by 19 and 18 pumping tests and an average absolute difference of around 6×10^{-3} was found. Correlation between the derived storage and the hydrogeological setting is observed. Where the chalk is overlain by the Lambeth Group and semi-confined conditions may persist the storage coefficient is typically 1×10^{-3} to 1×10^{-4}. Where the chalk is confined by the London Clay the storage coefficient is typically an order of magnitude lower and in the range 1×10^{-4} to 1×10^{-5}, though local geological effects associated with faulting and ground disturbance appear to have a bearing on these results and may warrant further investigation.

A 1-D model based on the approach proposed by Tomás et al. (2010) was implemented in order to simulate the ground motion response to hydraulic head changes in the semi-confined and confined aquifer conditions. The results of the modelling revealed that the ground response to groundwater levels variations is not uniform across the London Basin. Spatio-temporal variations of the storage coefficient are related to the groundwater levels with respect to the lithological units, and to the fractures network in the aquifer, which are believed to cause compartmentalisation of the aquifer. In those areas where the water level was found in the Lambeth Group, a greater storage coefficient (1×10^{-3}) than that measured where the water level was in the London Clay (3×10^{-4}–7×10^{-4}) was observed. The variability of the aquifer storage coefficient throughout the Basin as a consequence, requires different policies and zonal planning for certain parts of London to manage the available resource and conflicting aquifer uses effectively.

The modelling has also been useful in filling the temporal gap between ERS and ENVISAT PSI data. The ENVISAT ground motion time series were adjusted for the position of the ground on 13/12/2002 to match with the modelled ground motion time series based on the ERS data, and a vertical displacement of −5 mm was observed for piezometer 14149, 4 mm for piezometer 4979 and −2 mm for piezometer 14265.

In addition, the ground motion response to hydraulic head changes in the unconfined condition of the Chalk aquifer was analysed. The comparisons between the water table variations and the ground motion changes, located in the Chilterns Hills revealed that water table variations of around 2 m correspond to 4 mm in ground motion. Around five months of time lag between water table variations and ground motion changes were observed at two piezometers locations (piezometer 14795 and 14796). This time lag may be due to the presence of low saturated hydraulic conductivity deposits, which eventually delay the horizontal flow. However, there is insufficient evidence in the displacement time series to confirm this five month lag which could be simply due to intrinsic characteristics of the input satellite data and their temporal sampling (monthly to yearly). In the North Downs Chalk, the hydraulic head change of 20 m corresponds to approximately 3 mm of surface displacements.

We believe that the application of satellite data to understand the relationship between the groundwater levels and the surface displacements will provide new opportunities to inform future approaches for monitoring groundwater levels variations over wide urban areas, such as the London Basin and for wider spatial assessment of aquifer properties. The PSI-derived storage coefficient maps could be used within the London Basin aquifer model for groundwater resource sustainable management and for accurate simulation of artificial recharge operations. More widely, the findings of this work confirmed that PSI analysis and data are capable of supporting the characterisation of aquifer properties of fractured aquifers over wide regions of interest.

Acknowledgements

This study was carried out by R. Bonì in the framework of her PhD project at the University of Pavia and during her research visit at the British Geological Survey (BGS) in June-September 2015, under the supervision of F. Cigna and S. Bricker. ERS-1/2 and ENVISAT data were processed by H. McCormack in the framework of the EC-FP7 project PanGeo (http://www.pangeoproject.eu/). Groundwater level data were provided by the Environment Agency (Licence Agreement no. A2719; non-commercial use). The authors thank Dr Andrew Hughes for his insightful comments on the manuscript, and Mark Whiteman for providing the groundwater level data. F. Cigna and S. Bricker publish with the permission of the Executive Director of BGS-NERC.

References

Abbiss, C.P., 1979. A comparison of the stiffness of the chalk at Mundford from a seismic survey and a large scale tank test. Geotechnique 29 (4), 461–468.

Aldiss, D., Burke, H., Chacksfield, B., Bingley, R., Teferle, N., Williams, S., Blackman, D., Burren, R., Press, N., 2014. Geological interpretation of current subsidence and uplift in the London area, UK, as shown by high precision satellite-based surveying. Proc. Geol. Assoc. 125 (1), 1–13.

Aldiss, D.T., 2013. Under-representation of faults on geological maps of the London region: reasons, consequences and solutions. Proc. Geol. Assoc. 124 (6), 929–945.

Allen, D.J., Brewerton, L.J., Coleby, L.M., Gibbs, B.R., Lewis, M.A., MacDonald, A.M., Wagstaff, S.J., Williams, A.T., 1997. The Physical Properties of Major Aquifers in England and Wales. British Geological Survey Technical Report WD/97/34.

Balkhair, K.S., 2002. Aquifer parameters determination for large diameter wells using neural network approach. J. Hydrol. 265 (1), 118–128.

Banks, V.J., Bricker, S.H., Royse, K.R., Collins, P.E.F., 2015. Anomalous buried hollows in London: development of a hazard susceptibility map. Quart. J. Eng. Geol. Hydrogeol. 48 (1), 55–70. http://dx.doi.org/10.1144/qjegh2014-037.

Barker, J.A., 1991. Transport in fractured rock. In: Downing, R.A., Wilkinson, W.B. (Eds.), Applied Groundwater Hydrology. Clarendon Press, Oxford, pp. 199–216.

Bateson, L.B., Barkwith, A.K.A.P., Hughes, A.G., Aldiss, D.T., 2009. Terrafirma: London H-3 Modelled Product. Comparison of PS data with the results of a groundwater abstraction related subsidence Model. British Geological Survey Commissioned Report, OR/09/032, 47 pp.

Bell, F.G., 1977. A note on the physical properties of the chalk. Eng. Geol. 11 (3), 217–225.

Bell, J.W., Amelung, F., Ferretti, A., Bianchi, M., Novali, F., 2008. Permanent scatterer InSAR reveals seasonal and long-term aquifer-system response to groundwater pumping and artificial recharge. Water Resour. Res. 44 (2).

BGS, 2014. GeoSure: National Ground Stability Data Available at: <http://www.bgs.ac.uk/products/geosure/home.html>. (accessed on: 05/11/2015).

Bingley, R., Teferle, F.N., Orliac, E.J., Dodson, A.H., Williams, S.D.P., Blackman, D.L., Baker, T.F., Riedmann, M., Haynes, M., Aldiss, D.T., Burke, H.C., Chacksfield, B.C., Tragheim, D.G., 2007. Absolute Fixing of Tide Gauge Benchmarks and Land Levels: Measuring Changes in Land and Sea Levels around the coast of Great Britain and along the Thames Estuary and River Thames using GPS, Absolute Gravimetry, Persistent Scatterer Interferometry and Tide Gauges. Joint DEFRA/EA Flood and Coastal Erosion Risk Management R&D Programme. In: DEFRA/EA (Ed.), R&D Technical Report FD2319/TR: <http://nora.nerc.ac.uk/1493/1/Absolutefixing.pdf>.

Bloomfield, J.P., Brewerton, L.J., Allen, D.J., 1995. Regional trends in matrix porosity and dry density of the chalk of England. Quart. J. Eng. Geol. 28, S-131–S-142.

Bloomfield, J.P., Bricker, S.H., Newell, A.J., 2011. Some relationships between lithology, basin form and hydrology: a case study from the Thames basin, UK. Hydrol. Process. 25, 2518–2530. http://dx.doi.org/10.1002/hyp.8024.

Bonì, R., Herrera, G., Meisina, C., Notti, D., Béjar-Pizarro, M., Zucca, F., González, P.J., Palano, M., Tomás, R., Fernández, J., Fernández-Merodo, J.A., Mulas, J., Aragón, R., Guardiola-Albert, C., Mora, O., 2015. Twenty-year advanced DInSAR analysis of severe land subsidence: the Alto Guadalentín Basin (Spain) case study. Eng. Geol. 198, 40–52. http://dx.doi.org/10.1016/j.enggeo.2015.08.014.

Burbey, T.J., 2003. Use of time–subsidence data during pumping to characterize specific storage and hydraulic conductivity of semi-confining units. J. Hydrol. 281 (1), 3–22.

Carter, P.G., Mallard, D.J., 1974. A study of the strength, compressibility and density trends within the Chalk of southeast England. Quart. J. Eng. Geol. 7, 43–55.
Chaussard, E., Bürgmann, R., Shirzaei, M., Fielding, E.J., Baker, B., 2014. Predictability of hydraulic head changes and characterization of aquifer-system and fault properties from InSAR-derived ground deformation. J. Geophys. Res.: Solid Earth 119 (8), 6572–6590.
Cigna, F., Jordan, H., Bateson, L., McCormack, H., Roberts, C., 2015. Natural and anthropogenic geohazards in greater London observed from geological and ERS-1/2 and ENVISAT persistent scatterers ground motion data: results from the EC FP7-SPACE PanGeo Project. Pure Appl. Geophys. 172 (11), 2965–2995.
Cigna, F., Osmanoğlu, B., Cabral-Cano, E., Dixon, T.H., Ávila-Olivera, J.A., Garduño-Monroy, V.H., DeMets, C., Wdowinski, S., 2012. Monitoring land subsidence and its induced geological hazard with Synthetic Aperture Radar Interferometry: a case study in Morelia, Mexico. Remote Sens. Environ. 117, 146–161. http://dx.doi.org/10.1016/j.rse.2011.09.005.
Cooper, H.H., 1966. The equation of groundwater flow in fixed and deforming coordinates. J. Geophys. Res. 71 (20), 4785–4790.
De Freitas, M.H., 2009. Geology; its principles, practice and potential for Geotechnics. Quart. J. Eng. Geol. Hydrogeol. 42 (4), 397–441.
EA, 2007. Groundwater Levels in the Chalk-Basal Sands Aquifer of the London Basin. Unpublished report.
EA, 2015. Management of the London Basin Chalk Aquifer. Status Report 2015. Environment Agency of England and Wales, Thames Region Report.
Ellison, R.A., Woods, M.A., Allen, D.J., Forster, A., Pharaoh, T.C., King, C., 2004. Geology of London: special memoir for 1:50,000 geological sheets 256 (north London), 257 (Romford), 270 (south London), and 271 (Dartford) (England and Wales). British Geological Survey.
European Environment Agency, EEA, 2010. GMES Urban Atlas Available online at: <http://www.eea.europa.eu/data-and-maps/data/urban-atlas>. (accessed on: 05/11/2015).
Ezquerro, P., Herrera, G., Marchamalo, M., Tomás, R., Béjar-Pizarro, M., Martínez, R., 2014. A quasi-elastic aquifer deformational behavior: Madrid aquifer case study. J. Hydrol. 519, 1192–1204.
Ferretti, A., Prati, C., Rocca, F., 2001. Permanent scatterers in SAR interferometry. IEEE Trans. Geosci. Remote Sens. 39 (1), 8–20.
Fetter, C.W., 2001. Applied Hydrogeology, fourth ed. Prentice Hall, Upper Saddle River, p. 102, ISBN 0-13-088239-9.
Ford, J.R., Mathers, S.J., Royse, K.R., Aldiss, D.T., Morgan, D.J.R., 2010. Geological 3D modelling: scientific discovery and enhanced understanding of the subsurface, with examples from the UK. Z. Dtsch. Ges. Geowiss. 161, 205–218.
Freeborough, K., Kirkham, M., Jones, L.D., 2006. Determination of the shrinking and swelling properties of the London Clay Formation: laboratory report. British Geological Survey report IR/06/058, 34 pp.
Fry, V.A., 2009. Lessons from London: regulation of open-loop ground source heat pumps in central London. Quart. J. Eng. Geol. Hydrogeol. 42 (3), 325–334.
Gabriel, A.K., Goldstein, R.M., Zebker, H.A., 1989. Mapping small elevation changes over large areas: differential radar interferometry. J. Geophys. Res.: Solid Earth (1978–2012) 94 (B7), 9183–9191.
Galloway, D.L., Hoffmann, J., 2007. The application of satellite differential SAR interferometry-derived ground displacements in hydrogeology. Hydrogeol. J. 15 (1), 133–154.
Galloway, D.L., Hudnut, K.W., Ingebritsen, S.E., Phillips, S.P., Peltzer, G., Rogez, F., Rosen, P.A., 1998. Detection of aquifer system compaction and land subsidence using interferometric synthetic aperture radar, Antelope Valley, Mojave Desert, California. Water Resour. Res. 34 (10), 2573–2585.
Galloway, D., Jones, D.R., Ingebritsen, S.E. (Eds.), 1999. Land Subsidence in the United States. US Geological Survey, Reston, VA, USA, p. p. 177.
Helm, D.C., 1975. One-dimensional simulation of aquifer system compaction near Pixley, Calif. 1: constant parameters. Water Resour. Res. 11 (3), 465–478.
Helm, D.C., 1976. One-dimensional simulation of aquifer system compaction nearPixley, Calif. 2: stress-dependent parameters. Water Resour. Res. 1 (3), 375–391.
Herrera, G., Fernández, J.A., Tomás, R., Cooksley, G., Mulas, J., 2009. Advanced interpretation of subsidence in Murcia (SE Spain) using A-DInSAR data-modelling and validation. Nat. Hazards Earth Syst. Sci. 9 (3), 647–661.
Hoffmann, J., Galloway, D.L., Zebker, H.A., 2003. Inverse modeling of interbed storage parameters using land subsidence observations, Antelope Valley, California. Water Resour. Res. 39, 1031. http://dx.doi.org/10.1029/2001WR001252, 2.
Hoffmann, J., Zebker, H.A., Galloway, D.L., Amelung, F., 2001. Seasonal subsidence and rebound in Las Vegas Valley, Nevada, observed by Synthetic Aperture Radar Interferometry. Water Resour. Res. 37 (6), 1551–1566. http://dx.doi.org/10.1029/2000WR900404.
Hooper, A., Zebker, H., Segall, P., Kampes, B., 2004. A new method for measuring deformation on volcanoes and other natural terrains using InSAR persistent scatterers. Geophys. Res. Lett. 31 (23).
Hutchinson, J.N., 1980. Possible late Quaternary pingo remnants in central London. Nature 284 (5753), 253–255.
Jacob, C.E., 1940. On the flow of water in an elastic artesian aquifer. Eos, Trans. Am. Geophys. Union 21 (2), 574–586.
Jones, L., Terrington, R., 2011. Modelling volume change potential in the London Clay. Quart. J. Eng. Geol. Hydrogeol. 44, 109–122.
Jones, M.A., Hughes, A.G., Jackson, C.R., Van Wonderen, J.J., 2012. Groundwater resource modelling for public water supply management in London. Geol. Soc., London, Special Publ. 364 (1), 99–111.
Kaczmaryk, A., Delay, F., 2007. Interference pumping tests in a fractured limestone (poitiers–france): inversion of data by means of dual-medium approaches. J. Hydrol. 337 (1), 133–146.
Klemm, H., Quseimi, I., Novali, F., Ferretti, A., Tamburini, A., 2010. Monitoring horizontal and vertical surface deformation over a hydrocarbon reservoir by PSInSAR. First Break 28 (5).
Lewis, M.A., Jones, H.K., Macdonald, D.M.J., Price, M., Barker, J.A., Shearer, T.R., Wesselink, A.J., Evans, D.J., 1993. Groundwater storage in British aquifers: Chalk. National Rivers Authority R & D Note 128.
MacDonald, A.M., Allen, D.J., 2001. Aquifer properties of the Chalk of England. Quart. J. Eng. Geol. Hydrogeol. (November 2001) 34 (Part 4), 371–384.
Mason, P.J., Ghail, R.C., Bischoff, C., Skipper, J.A., 2015. Detecting and monitoring small-scale discrete ground movements across London, using Persistent Scatterer InSAR (PSI). In: XVI Geotechnical Engineering for Infrastructure and Development: XVI European Conference on Soil Mechanics and Geotechnical Engineering (ECSMGE). ICE Publishing, p. 9.
Massonnet, D., Rabaute, T., 1993. Radar interferometry: limits and potential. IEEE Trans. Geosci. Remote Sens. 31 (2), 455–464.
Mathers, S.J., Burke, H.F., Terrington, R.L., Thorpe, S., Dearden, R.A., Williamson, J.P., Ford, J.R., 2014. A geological model of London and the Thames Valley, southeast England. Proc. Geol. Assoc. 125 (4), 373–382.
Morris, B.L., Lawrence, A.R., Chilton, P.J., Adams, B., Calow, R.C., Klink, B.A., 2003. Groundwater and its susceptibility to degradation: A global assessment of the problem and options for Management. Early Warning and Assessment Report Series, RS.03-3. United Nations Environment Programme, Nairobi, Kenya.
Mortimore, R., Newman, T.G., Royse, K., Scholes, H., Lawrence, U., 2011. Chalk: its stratigraphy, structure and engineering geology in east London and the Thames Gateway. Quart. J. Eng. Geol. Hydrogeol. 44 (4), 419–444.
Newman, T., 2009. The impact of adverse geological conditions on the design and construction of the Thames Water Ring Main in Greater London, UK. Quart. J. Eng. Geol. Hydrogeol. 42, 5–21.
Notti, D., Mateos, R.M., Monserrat, O., Devanthéry, N., Peinado, T., Roldán, F.J., Fernández-Chacón, F., Galve, J.P., Lamas, F., Azañón, J.M., 2016. Lithological control of land subsidence induced by groundwater withdrawal in new urban areas (Granada Basin, SE Spain). Multiband DInSAR monitoring. Hydrol. Process.
NRFA, 2016. National River Flow Archive, 39001 Thames at Kingston. <http://nrfa.ceh.ac.uk/data/station/meanflow/39001> (accessed 10.02.2016).
O'Shea, M.J., Sage, R., 1999. Aquifer recharge: an operational drought-management strategy in North London. Water Environ. J. 13 (6), 400–405.
O'Shea, M.J., Baxter, K.M., Charalambous, A.N., 1995. The hydrogeology of the Enfield-Haringey artificial recharge scheme, north London. Quart. J. Eng. Geol. Hydrogeol. 28 (Suppl. 2), S115–S129.
Osmanoğlu, B., Dixon, T.H., Wdowinski, S., Cabral-Cano, E., Jiang, Y., 2011. Mexico City subsidence observed with persistent scatterer InSAR. Int. J. Appl. Earth Observ. Geoinform. 13 (1), 1–12.
Poland, J.F., 1984. Guidebook to Studies of Land Subsidence due to Ground-water Withdrawal. Unesco, Paris, France.
Price, M., 1987. Fluid flow in the Chalk of England. In: Goff, J.C., Williams, B.P.J. (Eds.), Fluid Flow in Sedimentary Basins and Aquifers, vol. 34. Geological Society London Special Publications,, pp. 141–156.
Price, M., Bird, M.J., Foster, S.S.D., 1976. Chalk pore-size measurements and their significance. Water Serv. October, 596–600.
Price, M., Downing, R.A., Edmunds, W.M., 1993. The Chalk as an aquifer. In: Downing, R.A., Price, M., Jones, G.P. (Eds.), The Hydrogeology of the Chalk of North-West Europe. Clarendon Press, Oxford, pp. 14–34.
Reeves, J.A., Knight, R., Zebker, H.A., Kitanidis, P.K., Schreüder, W.A., 2014. Estimating temporal changes in hydraulic head using InSAR data in the San Luis Valley, Colorado. Water Resour. Res. 50 (5), 4459–4473.
Riley, F.S., 1969. Analysis of borehole extensometer data from central California. In: Tison, L.J. (Ed.), Land subsidence. Proceedings of the Tokyo Symposium, September 1969, vol. 88. IAHS Pub., pp. 423–431. Available at: <http://iahs.info/redbooks/a088/088047.pdf>.
Riley, F.S., 1998. Mechanics of aquifer systems—The scientific legacy of Joseph F. Poland. In: Borchers, J.W. (Ed.), Land subsidence case studies and current research: Proceedings of the Dr. Joseph F. Poland Symposium on Land Subsidence: Belmont, Calif., Star Publishing Co., Association of Engineering Geologists Special Publication 8, pp. 13–27.
Royse, K.R., de Freitas, M., Burgess, W.G., Cosgrove, J., Ghail, R.C., Gibbard, P., King, C., Lawrence, U., Mortimore, R.N., Owen, H.G., Skipper, J., 2012. Geology of London, UK. Proc. Geol. Assoc. 123, 22–45.
Samieie-Esfahany, S., Hanssen, R., van Thienen-Visser, K., Muntendam-Bos, A., 2009. On the effect of horizontal deformation on InSAR subsidence estimates. In: Proceedings of The Fringe 2009 Workshop, vol. 30, Frascati, Italy.
Schad, H., Teutsch, G., 1994. Effects of the investigation scale on pumping test results in heterogeneous porous aquifers. J. Hydrol. 159 (1), 61–77.
Sneed, M., Galloway, D.L., 2000. Aquifer – System Compaction and Land Subsidence: Measurements, Analyses, and Simulations – the Holly Site, Edwards Air Force Base, Antelope Valley, California: U.S. Geological Survey Water-Resources Investigation Report 00-4015, 70p. Available online at <http://ca.water.usgs.gov/archive/reports/wrir004015/>.
Sumbler, M.G., 1996. British Regional Geology: London and the Thames Valley, fourth ed. HMSO for the British Geological Survey, London.
Terzaghi, K., 1943. Theory of Consolidation. John Wiley & Sons, Inc., pp. 265–296.
Thames Water, (Undated), Final Water Resources Management Plan 2015-2040, Executive Summary. Available online at: <https://www.thameswater.co.uk/

tw/common/downloads/wrmp/WRMP14_Section_0.pdf>. (accessed on 22 December 2015).
Tomás, R., Herrera, G., Cooksley, G., Mulas, J., 2011. Persistent scatterer interferometry subsidence data exploitation using spatial tools: the Vega media of the Segura River Basin case study. J. Hydrol. 400 (3), 411–428.
Tomás, R., Herrera, G., Delgado, J., Lopez-Sanchez, J.M., Mallorquí, J.J., Mulas, J., 2010. A ground subsidence study based on DInSAR data: calibration of soil parameters and subsidence prediction in Murcia City (Spain). Eng. Geol. 111 (1), 19–30.
Tomás, R., Lopez-Sanchez, J.M., Delgado, J., Mallorquí, J.J., 2006. Hydrological parameters of the Vega Media of the Segura River Aquifer (SE Spain) obtained by Means of Advanced DInSAR. In: Proceedings of the IEEE Intl. Geoscience and Remote Sensing Symposium, 2006. IGARSS 2006, vol. 3, pp. 1553–1556.
UK Groundwater Forum, 1998. Groundwater our Hidden Asset. British Geological Survey, Keyworth. Thames Water Authority, 1978. The Thames Groundwater Scheme. Institution of Civil Engineers, London.
Ward, W.H., Burland, J.B., Gallois, R.W., 1968. Geotechnical assessment of a site at Mundford, Norfolk, for a large proton accelerator. Geotechnique 18 (4), 399–431.
Werner, C., Wegmüller, U., Wiesmann, A., Strozzi, T., 2003. Interferometric point target analysis with JERS-1 L-band SAR data. In: Proceedings of the IEEE Intl. Geoscience and Remote Sensing Symposium, 2003. IGARSS 2003, vol. 7. IEEE, pp. 4359–4361.
Wolf, L., Morris, B., Burn, S., 2006. AISUWRS: Urban Water Resources Toolbox, 2006. IWA Publishing, London UK.